Influence of the ground state of the Ho^{3+} ions in orthochromites on their magnetic properties and phase transitions

I. A. Zorin, A. M. Kadomtseva, M. M. Lukina, and A. A. Mukhin

M. V. Lomonosov State University, Moscow

(Submitted 27 October 1986)
Zh. Eksp. Teor. Fiz. **93**, 266–273 (July 1987)

An investigation was made of the magnetic behavior of the Ising rare-earth Ho^{3+} ions in $HoCrO_3$ and $Ho_{0.07}Y_{0.93}CrO_3$ single crystals. Spontaneous and magnetic-field-induced orientational $\Gamma_4(G_xF_z) \rightleftarrows \Gamma_2(G_zF_x)$ transitions were observed in the dilute holmium orthochromite. Theoretical and experimental H_x–T and H_z–T phase diagrams were plotted and these were used to determine the main parameters of the system: the exchange splitting of the Ho^{3+} doublet ($2\Delta_{ex} = 15 \pm 0.5$ K), the weak ferromagnetic moments, and the anisotropy constants of the Cr subsystem. Anomalies in the field dependences of the magnetic and magnetoelastic properties were observed for the investigated compositions. These anomalies appeared in the course of unusual orientational ($\Gamma_2 \rightarrow \Gamma_4$) transitions in a field $\mathbf{H} \| \mathbf{b}$ and were due to crossing (approach) of the lower energy levels of the Ho^{3+} ions. A good agreement was obtained between the experimental and theoretical H_y–T phase diagrams.

1. INTRODUCTION

Holmium orthochromite ($HoCrO_3$) and other rare-earth orthochromites ($RCrO_3$) and orthoferrites ($RFeO_3$) crystallize in an orthorhombically distorted perovskite structure (space group D_{2h}^{16}-$Pbnm$).[1] An important role in the formation of magnetic properties of rare-earth orthochromites and orthoferrites is played by the nature of the ground state of the rare-earth ion (R^{3+}) in the crystal field and by its exchange interaction with the d subsystem (see, for example, Refs. 2 and 3). The ground multiplet of the Ho^{3+} ion ($^5I_8$), which is described by the point group C_s, is split into singlets by the crystal field in an orthochromite or an orthoferrite. The results of magnetic measurements on $HoCrO_3$ (Ref. 4) and $HoFeO_3$ (Ref. 5), and the results of optical investigations of $HoFeO_3$ (Ref. 6) have demonstrated that the ground state of the Ho^{3+} ion in these compounds is a quasidoublet (two closely spaced singlets), separated from the excited states by an interval ≈ 80 cm^{-1}, and the wave functions of this quasidoublet belong to two different irreducible representations of the group C_s. In this case the splitting of the quasidoublet is[3,7]

$$2\Delta^{\pm} = 2[\Delta_0^2 + (\Delta_{ex}G_z + \mathbf{m}_0^{\pm}\mathbf{H})^2]^{1/2}, \quad (1)$$

where $2\Delta_0$ and $2\Delta_{ex}$ represent the splitting in the crystal an exchange fields, respectively; $\mathbf{H}$ is the external magnetic field; $\mathbf{m}_0^{\pm}$ is the saturation value of the magnetic moment lying in the ab plane of a crystal at an angle $\pm\alpha$ to the a axis. The $\pm$ signs refer to two crystallographically inequivalent positions of the R^{3+} ion; $\mathbf{G}$ is the antiferromagnetic vector of the d subsystem ($|G| = 1$). Since the splitting of the ground quasidoublet of the Ho^{3+} ion in $HoCrO_3$ by the crystal field ($2\Delta_0$) is considerably less than its splitting in the exchange field ($\Delta_0 = 2 \pm 1$ K, $\Delta_{ex} = 7.4 \pm 0.1$ K),[4] it follows that ignoring Δ_0 we can regard Ho^{3+} with a high accuracy as an Ising ion with the magnetization axis along $\mathbf{m}_0^{\pm}$.

An important feature of the ground state of the Ho^{3+} ion is the strongly anisotropic nature of its splitting in the exchange field of the d subsystem. We can see from Eq. (1) that the exchange splitting occurs only when the antiferromagnetic vector $\mathbf{G}$ is tilted out of the ab plane of the crystal and reaches its maximum value in the $\Gamma_2(G_zF_x)$ phase, whereas in the $\Gamma_4(G_xF_z)$ and $\Gamma_1(G_y)$ phases the main quasidoublet is practically degenerate ($\mathbf{F}$ is the weak-ferromagnetism vector). Clearly, this is the reason why the $\Gamma_2(G_zF_x)$ phase appears in $HoCrO_3$ directly below $T_N = 140$ K (Ref. 4) in spite of the fact that the anisotropy energy of the Cr subsystem stabilizes the $\Gamma_4(G_xF_z)$ phase (as it does happen in $YCrO_3$—see Refs. 8 and 9). It should be pointed out that in the case of $HoFeO_3$, in which the exchange splitting of the quasidoublet of the Ho^{3+} ion is less than in $HoCrO_3$ [$\Delta_{ex}(HoFeO_3) = 4.9 \pm 0.3$ K is given in Ref. 10], the phase which appears directly below $T_N = 640$ K is $\Gamma_4(G_xF_z)$ and it is stabilized by the anisotropy energy of the Fe subsystem; cooling to $T \approx 60$ K results in reorientation to the $\Gamma_2(G_zF_x)$ phase. The mechanism of this phase transition is related to the improvement in the energy of the $\Gamma_2(G_zF_x)$ phase because of lifting of the degeneracy of the ground state of the Ho^{3+} ion[2,3] (this is the magnetic analog of the Jahn–Teller effect[11]).

Another interesting situation associated with the crossing (approach) of the lower energy levels of the Ho^{3+} ion occurs in a magnetic field $\mathbf{H} \| \mathbf{b}$. In this case the system acquires an instability manifested in the form of the $\Gamma_2 \rightarrow \Gamma_4$ ($G_zF_x \rightarrow G_xF_z$) orientational transition.[2,3] This reorientation has been observed experimentally in the form of anomalies on the magnetization curves of $HoFeO_3$ (Ref. 12) and by optical methods in the case of $HoCrO_3$ (Ref. 13).

These properties of the ground state of the Ho^{3+} ion in the structure of orthochromites and orthoferrites make these compounds extremely convenient objects for the investigation of the instability of the magnetic structure of the system due to a degenerate ground state of the rare-earth ion or due to crossing of its energy levels in a magnetic field.

Our aim was to investigate theoretically and experimentally, on the basis of magnetic and magnetostriction measurements, the exchange interactions, phase transitions, and H–T diagrams of pure orthochromite $HoCrO_3$ and of orthochromite $Ho_xY_{1-x}CrO_3$ diluted by Y^{3+} nonmagnetic

 0038-5646/87/070153-05$04.00

ions when $x = 0.07$. An investigation of the latter compound is of special interest, because this orthochromite should exhibit a spontaneous orientational transition $\Gamma_4 \rightarrow \Gamma_2$ (as in the case of $HoFeO_3$) at low values of x as well as a greater variety of magnetic transitions in an external field, which should provide extensive information on the magnetic interactions in the system.

2. EXPERIMENTS

Single crystals of $HoCrO_3$ and $Ho_{0.07}Y_{0.93}CrO_3$ grown from molten solutions were investigated by recording the magnetization isotherms along the *a*, *b*, and *c* axes of the crystal. Measurements were made using a vibrational magnetometer in the field of a superconducting solenoid up to 60 kOe at temperatures from 1.6 to 140 K. In the case of an $HoCrO_3$ single crystal the magnetostriction along the *b* axis was determined employing strain gauges at temperatures from 1.5 to 40 K in a superconducting solenoid (in fields up to 40 kOe). Figure 1(a) shows the low-temperature magnetization curves $HoCrO_3$ along the *a*, *b*, and *c* axes of an orthorhombic crystal (*x*, *y*, and *z* axes, respectively). We can see that the magnetization behaves very anisotropically; it saturates in high fields along the *a* and *b* axes, reaching approximate values 90 and 165 $G \cdot cm^3 \cdot g^{-1}$, respectively. The magnetization is minimal along the *c* axis and it varies practically linearly on increase in the field and the specific susceptibility is $\chi_c = 7 \times 10^{-4}$ cm^3/g. It is worth noting the

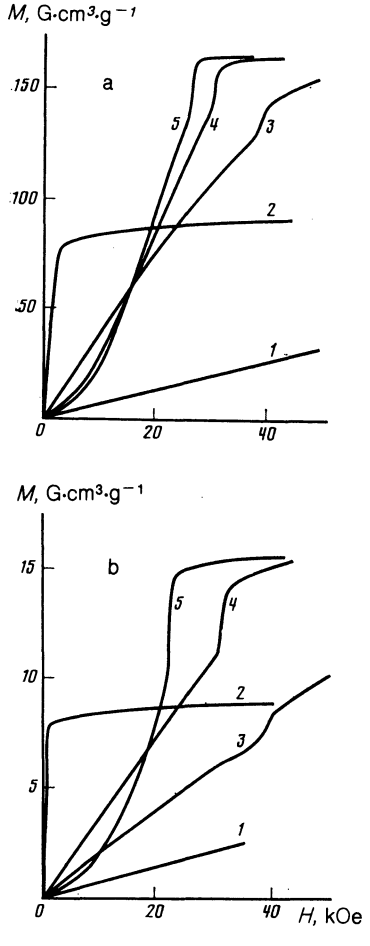

FIG. 1. a) Magnetization curves of $HoCrO_3$: 1) $T = 4.2$ K (**H**||**c**); 2) 4.2 K (**H**||**a**); 3) 7.5 K; 4) 4.2 K; 5) 1.68 K (**H**||**b**). b) Magnetization curves of $Ho_{0.07}Y_{0.93}CrO_3$: 1) $T = 4.2$ K (**H**||**c**); 2) 4.2 K (**H**||**a**); 3) 27.5 K; 4) 9.5 K; 5) 4.2 K (**H**||**b**).

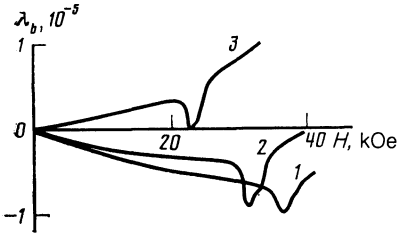

FIG. 2. Isotherms of magnetostriction λ_b obtained in a field **H**||**b** for $HoCrO_3$: 1) $T = 8.1$ K; 2) 6.5 K; 3) 4.2 K.

nature of the magnetization curves along the *b* axis, which exhibit a characteristic jump that shifts toward higher fields on increase in temperature. This jump corresponds to a reorientational $\Gamma_2 \rightarrow \Gamma_4$ transition similar to that occurring in $HoFeO_3$. Figure 2 shows that anomalies of the magnetostriction (λ_b) curves behave similarly in the case when **H**||**b**. The magnetostriction and magnetization data were used to plot the phase diagram (Fig. 3a).

Figure 1b shows the magnetization isotherms of an $Ho_{0.07}Y_{0.93}CrO_3$ crystal along the *a*, *b*, and *c* axes of a crystal at low temperatures. It is clear that the curves are similar to those of the other compounds, indicating that the behavior of the Ho^{3+} ions does not change greatly when some of them are replaced with Y^{3+}. The temperature dependence of the spontaneous magnetization of $Ho_{0.07}Y_{0.93}CrO$ is plotted in Fig. 4. As expected, in the case of this compound the Γ_4 phase appears at high temperatures directly below $T_N = 140$ K and cooling in the range 44–48 K induces a spontaneous reorientational transition $\Gamma_4 \rightarrow \Gamma_2$; the Γ_2 phase is retained right down to low temperatures. The application of a field along the *a* and *c* axes in a wide range of temperatures induces the $\Gamma_4 \rightarrow \Gamma_2$ and $\Gamma_2 \rightarrow \Gamma_4$ reorientational transitions, respectively. The corresponding threshold fields are shown in Fig. 5, the threshold fields **H**||**b** which induce the $\Gamma_2 \rightarrow \Gamma_4$ transition in this compound are plotted in Fig. 3b. It is worth noting that temperature rise converts an abrupt jump of the magnetization curves in the field **H**||**b** into a smooth inflection, indicating a change in the nature of the $\Gamma_2 \rightarrow \Gamma_4$ phase transition.

It should be pointed out that in the case of pure holmium orthochromite the application ofa field **H** = 60 kOe along the *c* axis did not induce the $\Gamma_2 \rightarrow \Gamma_4$ reorientational transitions throughout the investigated range of temperatures, which is evidence of a colossal anisotropy in the ac plane of $HoCrO_3$.

3. THEORY AND DISCUSSION OF RESULTS

The magnetic properties and phase transitions of $Ho_xY_{1-x}CrO_3$ compounds can be described using a simple one-doublet model in which the lower energy levels $E_i^{\pm}$ of the Ho^{3+} ions can be represented in the form

$$E_i^{\pm} = \Delta E_{VVi}(\mathbf{H}, \mathbf{G}, \mathbf{F}) \pm \Delta_i(\mathbf{H}, \mathbf{G}),$$

where the index $i = \pm$ distinguishes two inequivalent positions of the Ho^{3+} ions; Δ_i is described by Eq. (1), whereas ΔE_{VVi} (**H**, **G**, **F**) represents a shift of the center of gravity of the ground quasidoublet of the Ho^{3+} ion because of admixture of excited states as a result of the Ho–Cr exchange interaction and also because of the interaction with the external

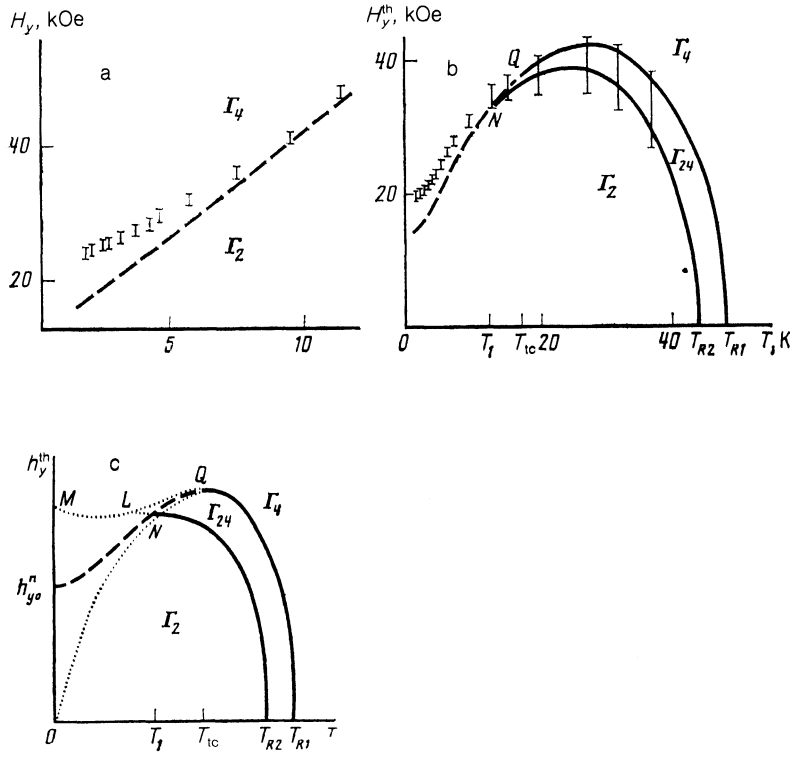

FIG. 3. Field-temperature (H_y–T) phase diagrams: a) $HoCrO_3$; b) $Ho_{0.07}Y_{0.93}CrO_3$; c) complete phase diagram of the system (shown schematically). The vertical segments represent the experimental values of the interval of the transition; the continuous curves represent second-order phase transition lines; the dashed curves are the first-order phase transition lines; the dotted lines represent the loss of stability.

field. The values of ΔE_{VVi}, calculated in the second order of perturbation theory, are the equivalent of the contribution to the energy of a magnetic material due to the Van Vleck paramagnetism (see, for example, Refs. 2 and 3). Without specifying the explicit form of ΔE_{VVi}, we shall include them below by renormalization of the coefficients of the thermodynamic potential of the Cr subsystem and refer to them as the Van Vleck contribution.

The thermodynamic potential of such a system (calculated per molecule) can be represented in the form[2,3]

$$\Phi(\theta) = \tilde{\Phi}_{Cr} - \frac{1}{2}\varkappa T \sum_{i=\pm} \ln 2\,\mathrm{ch}\left(\frac{\Delta_i(\theta)}{T}\right). \qquad (2)$$

where θ is the angle which defines the orientation of the antiferromagnetic vector $\mathbf{G} = (\sin\theta,\ 0,\ \cos\theta)$ in the ac plane relative to the c axis;

$$\tilde{\Phi}_{Cr}(\theta) = \Phi_{Cr}(\theta) + \frac{1}{2}\varkappa \sum_{i=\pm} E_{B\Phi i}(\theta) = \frac{1}{2}K_1\cos^2\theta + \frac{1}{4}K_2\cos^4\theta - m_x^0 H_x\cos\theta - m_z^0 H_z\sin\theta - \frac{1}{2}\varkappa\sum_{\alpha=x,y,z}\chi_{B\Phi}^{\alpha}H_\alpha^2 - \frac{1}{2}\chi_\perp^{Cr}[H^2-(\mathbf{HG})^2] \qquad (3)$$

is the thermodynamic potential of the Cr subsystem minimized with respect to **F** and renormalized by the Van Vleck contribution ΔE_{VVi} to the ground state of the Ho^{3+} ion: $K_1 = K_1^{Cr} + \varkappa K_1^{VV}$, $m_{x,z}^0 = m_{x,z}^{Cr} + \varkappa m_{x,z}^{VV}$. The last term in Eq. (3) will be ignored because it is unimportant in the effects under discussion.

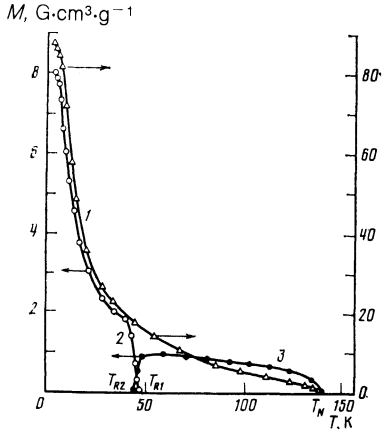

FIG. 4. Temperature dependences of the spontaneous magnetic moments: 1) m_x ($HoCrO_3$); 2) m_x; 3) m_z ($Ho_{0.07}Y_{0.93}CrO_3$).

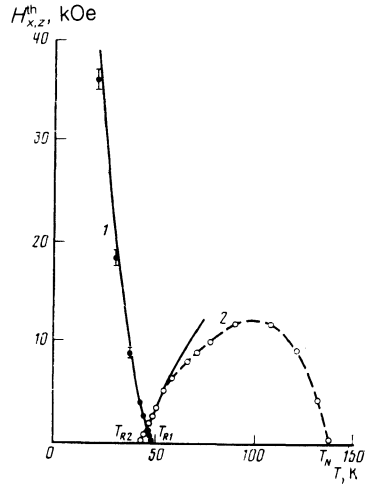

FIG. 5. Temperature dependences of the threshold fields of $Ho_{0.07}Y_{0.93}CrO_3$: 1) H_z^{th}; 2) H_x^{th}. The points are the experimental values and the continuous curves are theoretical.

We shall also ignore at this stage the small splitting in the crystal field (Δ_0), which occurs in Eq. (1), but we shall discuss its role briefly later.

We shall begin by using the experimental magnetization curves obtained along the a and b axes to find the main characteristics of the Ho^{3+} ion: the magnetic saturation moment m_0 and the orientation of the Ising axis (angle α). In the case of $\varkappa = 1$ and $\varkappa = 0.07$ these quantities are practically the same and equal to $m_0 = (8.6 \pm 0.2)\mu_B$, $\alpha = 62 \pm 1°$. These values are in good agreement with the results obtained for $HoCrO_3$ in Ref. 4: $m_0 = (8.7 \pm 0.15)\mu_B$, $\alpha = 65 \pm 1°$.

The temperature dependence of the spontaneous weak ferromagnetic moment along the a axis in the $\Gamma_2(\theta = 0)$ phase can be obtained from Eq. (2):

$$m_x = m_x^0 + \varkappa m_0 \cos\alpha \,\mathrm{th}(\Delta_{ex}/T). \tag{4}$$

The experimental dependence $m_x(T)$ recorded for $Ho_{0.07}Y_{0.93}CrO_3$ (Fig. 4) is described by Eq. (4) if we assume that $m_x^0 = (0.010 \pm 0.002)\mu_B$ and $\Delta_{ex} = 7.5$ K, in good agreement with the results of Ref. 4.

We shall now discuss spontaneous orientational transitions of the $\Gamma_4 \to \Gamma_{42} \to \Gamma_2$ type which occur in $Ho_\varkappa Y_{1-\varkappa}CrO_3$ ($\varkappa = 0.07$) at temperatures $T_{R1} = 48$ K and $T_{R2} = 44$ K, respectively (Fig. 4). The condition of stability of the corresponding phases $(\partial^2\Phi/\partial\theta^2) \geqslant 0$ yields the following expressions for the transition temperatures:

$$T_{R1} = \frac{\varkappa\Delta_{ex}^2}{K_1}, \quad T_{R2} = \frac{\Delta_{ex}}{\mathrm{arth}[(K_1+K_2)/\varkappa\Delta_{ex}]} = \frac{\varkappa\Delta_{ex}^2}{K_1+K_2}. \tag{5}$$

We shall now analyze the behavior of the system in a magnetic field.

a) H||c. This field induces an orientational transition from the Γ_2 phase to Γ_4. The threshold field found from the condition $(\partial^2\Phi/\partial\theta^2)_{\theta=\pi/2} = 0$ is

$$H_z^{th} = \frac{\varkappa\Delta_{ex}^2}{m_z^0}\left(\frac{1}{T} - \frac{1}{T_{R1}}\right). \tag{6}$$

The experimental results give $m_z^0 = 0.036\mu_B$. It should be pointed out that the lower value of m_z^0 for this composition compared with the value for $YCrO_3$ ($m_z^{Cr} = 0.047\mu_B$ is given in Ref. 8) clearly demonstrates that the Van Vleck contribution (m_z^{VV}) of the Ho^{3+} ions to the magnetization along the c axis is negative.

b) H||a. This field induces the $\Gamma_4 \to \Gamma_2$ orientational transition in $Ho_{0.07}Y_{0.93}CrO_3$ at temperatures $T > T_{R2}$. The threshold field is described by analogy with the preceding case, bearing in mind that $\Delta_{ex} \ll T_{R2}$:

$$H_x^{th} = \frac{\varkappa\Delta_{ex}^2}{m_x(T)}\left(\frac{1}{T_{R2}} - \frac{1}{T}\right), \tag{7}$$

where $m_x(T) \approx m_x^0 + \varkappa m_0(\Delta_{ex}/T)\cos\alpha]$ see [Eq. (4)]. Figure 5 shows the temperature dependences $H_z^{th}(T)$ and $H_x^{th}(T)$, calculated for $\Delta_{ex} = 7.5$ K, which at temperatures $T < 80$ K agree well (within the limits of the adopted approximation) with the experimental results, confirming the correctness of the selected model.

We shall use Eq. (5) to estimate the anisotropy constants K_1 and K_2:

$$K_1 = \varkappa\Delta_{ex}^2/T_{R1} = 0.084 \text{ K}, \quad K_2 = K_1(T_{R1}/T_{R2} - 1) = 0.08K_1. \tag{8}$$

The value of K_1 given above differs somewhat from the corresponding anisotropy constant of $YCrO_3$ (Refs. 8 and 9) which amounts to $K_1(YCrO_3) = 0.17$ K. The difference between K_1 for $\varkappa = 0.07$ from $K_1(YCrO_3)$ is obviously due to the Van Vleck contribution of the Ho^{3+} ions to K_1.

In the case of the constant K_2 we know that in orthochromites the Cr subsystem makes no contribution to this constant ($S_{Cr} = 3/2$). However, in this case the nonzero value of K_2, ensuring a finite interval of spin reorientation in $Ho_{0.07}Y_{0.93}CrO_3$, is due to a fluctuation mechanism associated with the inhomogeneity of the distribution of the Ho^{3+} ions in a crystal (Ref. 14).

c) H||b. This case is interesting and more complex.

In both preceding cases a field-induced orientational transition is associated with the interaction between **H** and the corresponding component of the weak ferromagnetic moment (m_x or m_z), whereas in the **H||b** case the situation is qualitatively different because there is no weak ferromagnetic moment along the b axis. In this case an important role is played by the effect of the external field on the splitting of the ground quasidoublet of the Ho^{3+} ion. According to Eq. (1), in the case of the $\Gamma_2(G_zF_x)$ phase subjected to the field **H||b** this splitting rises for some positions and decreases for others. In the region of crossing (approach) of the lower energy levels of the Ho^{3+} ions in the system, it follows from Refs. 3 and 11 that an instability of the magnetic structure of the d subsystem appears and it tends to produce an additional repulsion between the levels. In our case this instability is manifested by the $\Gamma_2 \to \Gamma_4$ orientational transition and by an abrupt change of the curves representing the magnetization along the b axis, which is due to reversal of the magnetization of the Ho^{3+} ions at one of the inequivalent positions.

The field inducing the first-order $\Gamma_2 \to \Gamma_4$ phase transition can be found by equating the thermodynamic potentials of the two phases. At $T = 0$ this field is

$$h_{y0}^{th} \equiv H_{y0}^{th} m_0 \sin\alpha = \Delta_{ex} - k/2, \tag{9}$$

whereas at finite temperatures we have

$$h_y^{th}(T) = \frac{T}{2}\,\mathrm{arch}\left[\frac{\mathrm{ch}(2\Delta_{ex}/T) - \exp(k/T)}{\exp(k/T) - 1}\right], \tag{10}$$

where $k = (K_1 + \frac{1}{2}K_2)/\varkappa$.

The complete h_y–T phase diagram of the system obtained from an analysis of the thermodynamic potential (2) is shown schematically in Fig. 3c. We can see that an increase in temperature changes the nature of spin reorientation and in the range $T > T_1$ it involves a series of two phase transitions $\Gamma_2 \to \Gamma_{42} \to \Gamma_4$. The first of these transitions occurs smoothly, whereas the second is a first-order transition if $T < T_{tc}$ and a second-order transition if $T > T_{tc}$. The equations describing the phase transition lines QT_{R1} and NT_{R2} are given by the following formulas:

$$h_y = T\,\mathrm{arth}(1 - TK_1/\Delta_{ex}^2\varkappa), \tag{11}$$

$$h_y = T\,\mathrm{arth}\left[\frac{1 - \eta\,\mathrm{cth}(\Delta_{ex}/T)}{1 - \eta\,\mathrm{th}(\Delta_{ex}/T)}\right], \tag{12}$$

where $\eta = (K_2 + K_1)/\Delta_{ex}\varkappa$.

The temperature corresponding to the tricritical point Q is

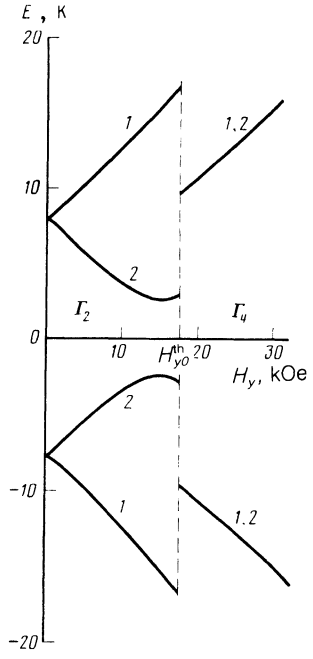

FIG. 6. Behavior of the energy levels of the ground quasidoublet of the Ho^{3+} ions in $HoCrO_3$ at the $\Gamma_2 \rightarrow \Gamma_4$ phase transition in a field $\mathbf{H}\|\mathbf{b}$ ($T=0$): 1) "+" position; 2) "−" position.

$$T_{tc} = \frac{K_1^2}{2\varkappa K_2}\left[\left(1+\frac{8K_2\Delta_{ex}^2\varkappa^2}{3K_1^3}\right)^{1/2}-1\right], \qquad (13)$$

and we also have $T_1 \lesssim T_{tc}$ when $\eta \ll 1$, which is well satisfied in our case.

Comparing the theoretical (Fig. 3c) and experimental (Figs. 3a and 3b) phase diagrams, we note that they are in good qualitative agreement. This applies particularly to the system $Ho_{0.07}Y_{0.93}CrO_3$ for which a fuller temperature dependence of the threshold field was determined experimentally. A numerical calculation of the H_y–T phase diagrams for both compounds with $\varkappa = 0.07$ and $\varkappa = 1$ gives results which are in quite satisfactory agreement with the experimental diagrams also in the quantitative sense (Figs. 3a and 3b). We calculated these diagrams assuming the following values of the parameters: $\Delta_{ex} = 7.5$ K, $m_0 = 8.6\mu_B$, $\alpha = 62°$; $K_1 = 0.40$ K and $K_2 = 0$ for $HoCrO_3$; $K_1 = 0.084$ K and $K_2 = 0.007$ K for $Ho_{0.07}Y_{0.93}CrO_3$.

It is interesting to note that the low-temperature value of the threshold fields of $HoCrO_3$ and $Ho_{0.07}Y_{0.93}CrO_3$ are similar. This is due to the fact that in this range of temperatures the threshold field is determined mainly by the quantity Δ_{ex}, as can be deduced from Eqs. (9) and (10), and the latter quantity exceeds considerably $k/2$ and gives for the above parameters $H_{y0}^{th} \approx 14$ kOe. The difference between this value of H_{y0}^{th} and the experimental threshold field (≈ 20 kOe) is clearly due to the neglect of the splitting Δ_0 in the crystal field and of the R–R interaction, and also due to possible experimental errors.

Allowance for the crystal field splitting (assuming that $\Delta_0 = 2.5$ K) gives at $T = 0$ the value

$$H_{y0}^{th} \approx (\Delta_{ex}+\tfrac{1}{2}\Delta_0 - k/2)/m_0 \sin\alpha \approx 16.2 \text{ kOe} \qquad (14)$$

for the composition with $\varkappa = 0.07$ and ≈ 16.5 kOe for $\varkappa = 1$. A numerical calculation shows that at finite temperatures if $T \gtrsim \Delta_0$ the phase diagram is practically the same as that obtained in the case when $\Delta_0 = 0$.

The splitting in the crystal field has a greater influence on the behavior of the lower energy levels of the Ho^{3+} ions in the region where these levels approach one another. Figure 6 shows the behavior of the lower levels of the Ho^{3+} ions in $HoCrO_3$ at $T = 0$ in the course of the $\Gamma_2 \rightarrow \Gamma_4$ transition in a field $\mathbf{H}\|\mathbf{b}$ (calculated allowing for the crystal field), which is in good agreement with the results of optical investigations.[13]

4. CONCLUSIONS

We shall now summarize the main results of the present investigation. It follows from magnetic measurements that Ho^{3+} in $HoCrO_3$ and $Ho_{0.07}Y_{0.93}CrO_3$ behaves as an Ising ion with the saturation value of the magnetic moment $m_0 = 8.6\mu_B$ and the easy magnetization axis lying in the ab plane at an angle $\alpha = 62°$ to the a axis.

Spontaneous and magnetic-field-induced orientational phase transitions occur in $Ho_{0.07}Y_{0.93}CrO_3$. We plotted theoretical and experimental H–T phase diagrams and used them to determine the exchange splitting of the ground quasidoublet of the Ho^{3+} ion amounting to $2\Delta_{ex} = 15 \pm 0.5$ K the effective weak ferromagnetic moments of the Cr subsystem $m_z^0 = 0.036\mu_B$ and $m_x^0 = 0.010\mu_B$ (at $T \ll T_N$), and the effective anisotropy constants of the Cr subsystem $K_1 = 0.084$ K and $K_2 = 0.007$ K.

The characteristic orientational transitions in a field $\mathbf{H}\|\mathbf{b}$ were analyzed in detail for both compositions. These transitions were associated with the crossing (approach) of the lower energy levels of the Ho^{3+} ions. We calculated the corresponding H_y–T phase diagrams, which are in good agreement with the experimental results.

[1] M. Marezio, J. P. Remeika, and P. D. Dernier, Acta Crystallogr. Sect. B **26**, 2008 (1970).
[2] K. P. Belov, A. K. Zvezdin, A. M. Kadomtseva, and R. Z. Levitin, *Orientational Transitions in Rare-Earth Magnetic Materials* [in Russian], Nauka, Moscow (1979).
[3] A. K. Zvezdin, V. M. Matveev, A. A. Mukhin, and A. I. Popov, *Rare-Earth Ions in Magnetically Ordered Crystals* [in Russian], Nauka, Moscow (1985).
[4] R. M. Hornreich, V. M. Wanklyn, and I. Yaeger, Int. J. Magn. **2**, 77 (1972).
[5] A. Apostolov, A. de Combarieu, A. Kappatsh, *et al.*, Colloq. Int. C.N.R.S., Grenoble **2**, 403 (1970).
[6] H. Schuchert, S. Hüfner, and R. Faulhaber, Z. Phys. **220**, 280 (1969).
[7] A. P. Malozemoff, J. Phys. Chem. Solids **32**, 1669 (1971).
I. S. Jacobs, F. Burne, and L. M. Levinson, J. Appl. Phys. **42**, 1631 (1971).
[9] A. M. Kadomtseva, A. P. Agafonov, M. M. Lukina, V. N. Milov, A. S. Moskvin, V. A. Semenov, and E. V. Sinitsyn, Zh. Eksp. Teor. Fiz. **81**, 700 (1981) [Sov. Phys. JETP **54**, 374 (1981)].
[10] J. C. Walling and R. L. White, Phys. Rev. B **10**, 4737 (1974).
[11] A. K. Zvezdin, A. A. Mukhin, and A. I. Popov, Pis'ma Zh. Eksp. Teor. Fiz. **23**, 267 (1976) [JETP Lett. **23**, 240 (1976)].
[12] Y. Allain, J. E. Bouree, J. Denis, J. Wajnflasz, and M. Lecomte, J. Phys. (Paris) **32**, Colloq. 1, C1-494 (1971).
[13] N. Kojima, I. Tsujikawa, K. Aoyagi, and K. Tsushima, J. Phys. Soc. Jpn. **54**, 4804 (1985).
[14] E. V. Sinitsyn and I. G. Bostrem, Zh. Eksp. Teor. Fiz. **85**, 661 (1983) [Sov. Phys. JETP **58**, 385 (1983)].

Translated by A. Tybulewicz